

LASER INTERFEROMETER GRAVITATIONAL WAVE OBSERVATORY  
- LIGO -  
CALIFORNIA INSTITUTE OF TECHNOLOGY  
MASSACHUSETTS INSTITUTE OF TECHNOLOGY

Technical Note	LIGO-T1000242-v1	Date: 9/19/2010
<h1>Hierarchical Control Theory for Advanced LIGO</h1>		
Brett Shapiro		

California Institute of Technology  
LIGO Project, MS 18-34  
Pasadena, CA 91125  
Phone (626) 395-2129  
Fax (626) 304-9834  
E-mail: info@ligo.caltech.edu

Massachusetts Institute of Technology  
LIGO Project, Room NW22-295  
Cambridge, MA 02139  
Phone (617) 253-4824  
Fax (617) 253-7014  
E-mail: info@ligo.mit.edu

LIGO Hanford Observatory  
Route 10, Mile Marker 2  
Richland, WA 99352  
Phone (509) 372-8106  
Fax (509) 372-8137  
E-mail: info@ligo.caltech.edu

LIGO Livingston Observatory  
19100 LIGO Lane  
Livingston, LA 70754  
Phone (225) 686-3100  
Fax (225) 686-7189  
E-mail: info@ligo.caltech.edu

## Contents

<b>1</b>	<b>Introduction</b>	<b>2</b>
<b>2</b>	<b>SISO Control Review</b>	<b>2</b>
<b>3</b>	<b>Hierarchical Control Theory</b>	<b>5</b>
3.1	Two Input Case . . . . .	5
3.2	Generalization to N Inputs . . . . .	11

## 1 Introduction

Given the quantity of multi-stage suspensions planned for Advanced LIGO, hierarchical control loops will be everywhere. Naturally, it is worth thoroughly understanding all the subtleties of designing such loops. For Advanced LIGO the term ‘hierarchical control’ typically references the active feedback applied to the various stages of multi-stage suspensions to control the position of the bottom stage for maintaining lock in a cavity.

Stability theory for linear single-input-single-output (SISO) systems is well developed and straight forward. While hierarchical control is not SISO, rather MISO (multi-input-single-output), SISO stability theory can be extended to this MISO case. Section 2 briefly reviews SISO systems by the example of maintaining lock in a cavity by actuating on the test mass of a quadruple pendulum. Section 3 introduces hierarchical control by following the same example but with additional actuation at multiple stages of the quadruple pendulum. It will be shown that although the stability criteria of MISO systems are the same as those for SISO systems, there are subtleties to consider. Suggestions on how to handle these subtleties to simplify design and robustify practical implementation are given.

Some knowledge of, block diagrams, bode plots, phase margin, and gain margin is assumed.

## 2 SISO Control Review

First, we review regular SISO stability criteria in the Fabry-Perot cavity locking example below. In this example we maintain a precise cavity length by actuating on just the bottom stage of a quadruple pendulum. Figure 1 illustrates a schematic diagram of this control loop. In block diagram form this looks like Figure 2.

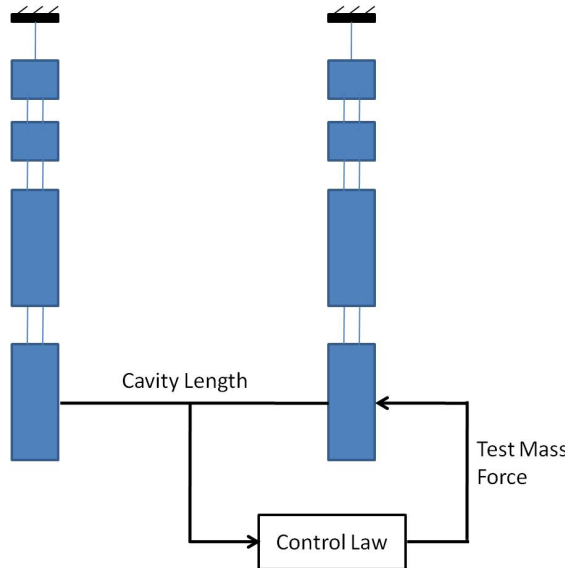


Figure 1: A schematic drawing of a SISO Fabry-Perot cavity loop that actuates only the bottom mass of a quad.

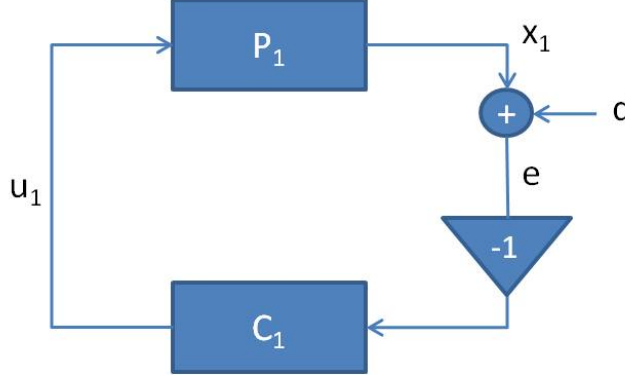


Figure 2: A block diagram of the SISO cavity loop in Figure 1.  $P_1$  is the quad transfer function from test mass force to test mass position,  $C_1$  the test mass feedback controller,  $x_1$  the test mass position,  $d$  the position of the opposing mirror (also other noise terms as well),  $e$  the measured cavity error, and  $u_1$  the force applied to the test mass.

The closed loop transfer function  $M_1$  from the disturbance  $d$  (opposing mirror position, measurement noise, etc) to the measured cavity signal  $e$  is calculated as follows

$$e = d + x_1 \quad (1)$$

$$x_1 = -C_1 P_1 e \quad (2)$$

$$e = d - C_1 P_1 e \quad (3)$$

$$M_1 = \frac{e}{d} = \frac{1}{1 + C_1 P_1} \quad (4)$$

The relative stability of the closed loop system is determined by the proximity of the open loop transfer function  $C_1 P_1$  to  $C_1 P_1 = -1$ . Consequently, a  $C_1$  that provides good stability margins around this point, known as phase margin and gain margin, will avoid large oscillations and guarantee robustness. These margins are highlighted below with the design of a simple loop to lock this cavity.

For the design of this loop, the quad's transfer function  $P_1$  from actuation at the test mass to the position of the test mass along the cavity axis is shown in Figure 3. To sufficiently reduce the error signal and maintain good locking we need to make the closed loop transfer function  $M_1$  very small where the disturbance  $d$  is highest. Since the majority of the disturbance is seismic noise, this means we need a large open loop transfer function  $C_1 P_1$  at low frequencies.

To get high gain at low frequencies while leaving sufficient stability margins,  $C_1$  is chosen with a zero at 50 Hz and two poles at 500 Hz. The gain is adjusted so that the  $C_1 P_1$  crosses magnitude 1 at 100 Hz. See the Bode plot of  $C_1 P_1$  in Figure 4. The phase margin is about 40 degrees and the gain margin is 8.59. These are fairly robust margins as can be seen by the lack of gain peaking around the 100 Hz unity gain crossover in the closed loop Bode plot of  $M_1$  in Figure 5.

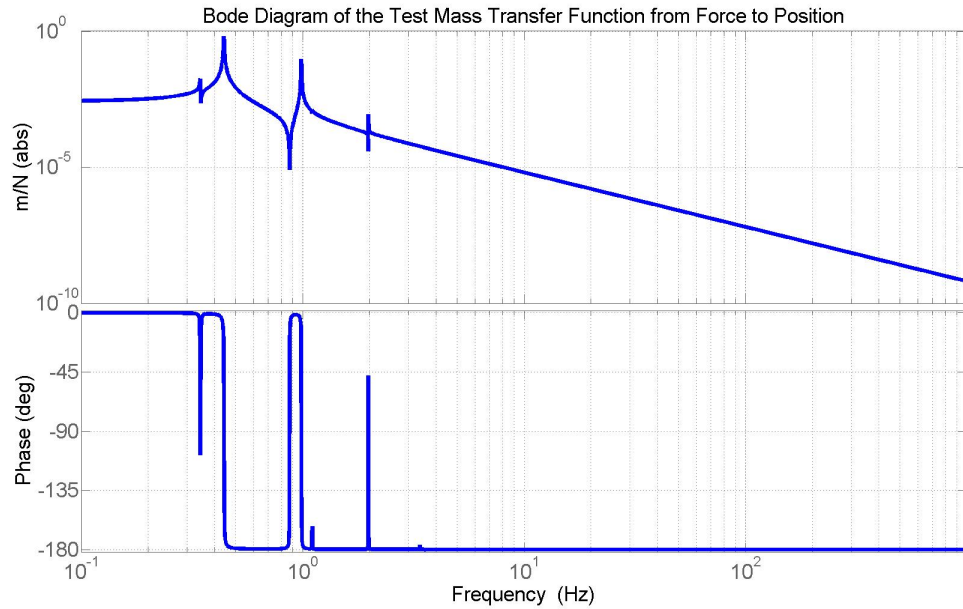


Figure 3: The quad transfer function  $P_1$  from a test mass force to the test mass position along the cavity axis.

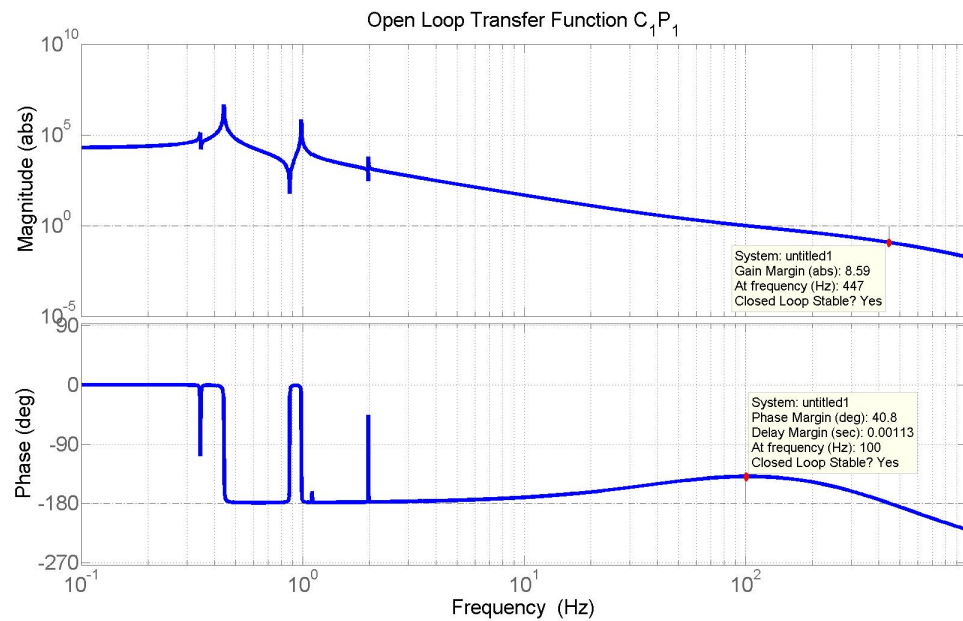


Figure 4: The open loop transfer function  $C_1 P_1$  from the error signal  $e$  to test mass position  $x_1$ .

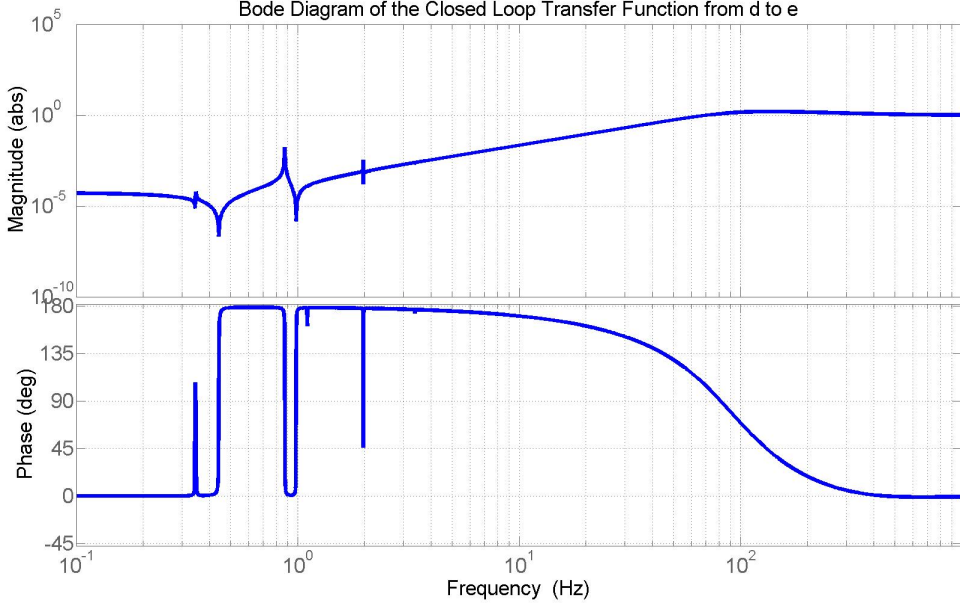


Figure 5: The closed loop transfer function  $M_1$  from the disturbance  $d$  to error signal  $e$  for the loop gain in Figure 4. Any disturbances or noise below 100 Hz will be attenuated.

### 3 Hierarchical Control Theory

As mentioned before, there are some subtleties that must be considered while extending SISO rules to multi-input feedback loops. The main subtlety being the addition of stability margins where the gain of multiple loops cross each other. This section introduces hierarchical control theory through the simple two input example below before generalizing the theory to arbitrary numbers of inputs.

#### 3.1 Two Input Case

To see how hierarchical control works, let's expand the SISO example from Section 2 to include feedback to the penultimate mass. The updated schematic is shown in Figure 6. The updated block diagram is given in Figure 7.

In fact, there are now two ways to draw the block diagram for this loop. Figure 8 highlights this point. The left side of this figure is just a copy of Figure 7, which shows a parallel feedback scheme. The error signal is passed to a controller for each stage simultaneously, which then actuates on its respective stage. The right side shows a nested scheme. An ‘inner’ loop is the closed loop system with feedback to just the test mass, just like in the SISO example. This inner system then becomes the plant of the penultimate mass controller. Both these representations are equivalent, but keeping them both in mind helps understand the additional stability considerations.

Considering the parallel representation we can develop the overall closed loop transfer function,  $M_2$ , for the entire feedback system.

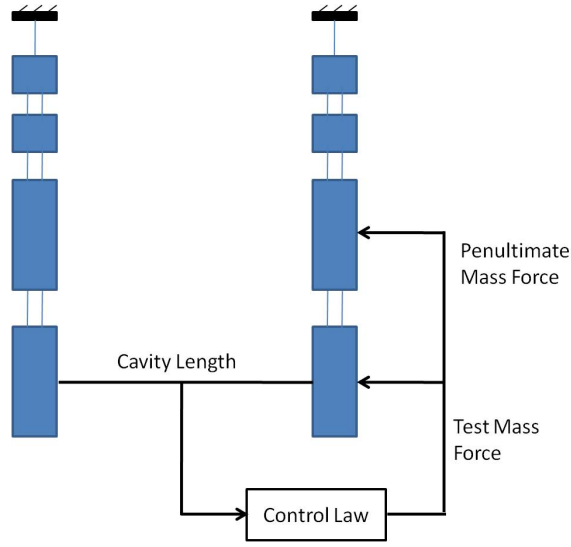


Figure 6: A schematic drawing of a hierarchical cavity loop that actuates both the bottom mass and penultimate mass of a quad.

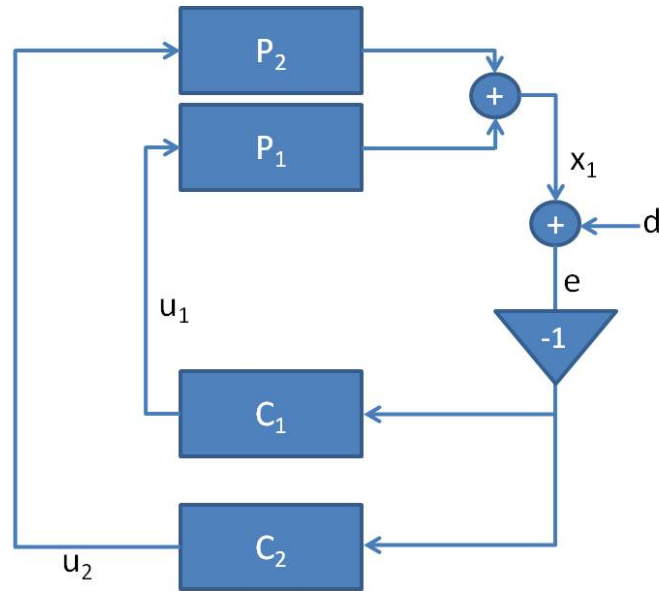


Figure 7: A block diagram of the hierarchical cavity loop in Figure 6.  $P_1$  is the quad transfer function from test mass force to test mass position,  $P_2$  is the quad transfer function from penultimate mass force to test mass position,  $C_1$  the test mass feedback controller,  $C_2$  the penultimate mass feedback controller,  $x_1$  the test mass position,  $d$  the position of the opposing mirror (also other noise terms as well),  $e$  the measured cavity error,  $u_1$  the force applied to the test mass, and  $u_2$  the force applied to the penultimate mass.

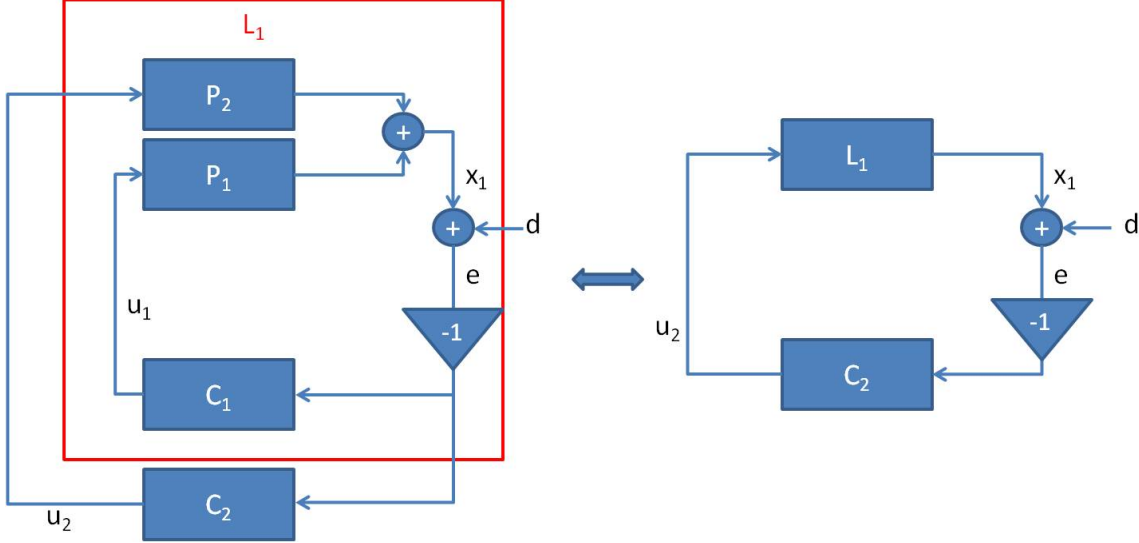


Figure 8: The block diagram in Figure 7 has two equivalent representations. The left shows parallel feedback while the one on the right shows nested feedback. In nested feedback, the test mass loop is controlled first. This ‘inner’ loop becomes the plant for the penultimate mass controller. These representations are merely conceptual and have no impact on the physics of the problem.

$$e = d - (C_1 P_1 + C_2 P_2) e \quad (5)$$

$$M_2 = \frac{e}{d} = \frac{1}{1 + C_1 P_1 + C_2 P_2} \quad (6)$$

From the Eq. 6 we see that stability is determined from the point

$$C_1 P_1 + C_2 P_2 = -1 \quad (7)$$

This stability criterion is just like that of the SISO case except that now we are summing the open loop transfer functions for the control of each individual stage. Care must be taken however, because with the additional terms there are many more ways to approach this  $-1$  point. One way is for one term to be small while the other approaches  $-1$ . Another way to reach  $-1$  is for both loops to be very large with similar magnitudes but opposite phase. For example, let’s rewrite Eq. 7 as

$$\frac{C_2 P_2}{1 + C_1 P_1} = -1 \approx \frac{C_2 P_2}{C_1 P_1} \quad (8)$$

$$\text{where, } |C_1 P_1| \gg 1 \quad (9)$$

Writing the stability as shown in Eq. 8 is important because it tells us that we must consider stability when two loop gains that are greater than magnitude 1 cross each other.

This loop crossover stability issue is even more readily derived from the nested loop representation. The inner loop has the transfer function

$$L_1 = P_2 M_1 = \frac{P_2}{1 + C_1 P_1} \quad (10)$$

The overall closed loop transfer function then becomes

$$M_2 = \frac{M_1}{1 + C_2 L_1} \quad (11)$$

$$M_2 = \frac{\frac{1}{1 + C_1 P_1}}{1 + \frac{C_2 P_2}{1 + C_1 P_1}} \quad (12)$$

Eq. 12 reconstructs the form of the stability criterion given by 8. Multiplying the top and bottom of 12 by the inverse of the numerator brings us back to the original form of  $M_2$  in Eq. 6.

Let's now try designing controllers to feedback to both these stages. Since we already have a working controller for the test mass from Section 2 we will keep that for the test mass here. We would like to use the PUM to increase the low frequency open loop gain to suppress the seismic noise even more. A simple and naive filter to do this is to simply give the PUM an integrator, i.e. a  $C_2$  with just pole at 0 Hz. Figure 9 plots the open loop transfer functions for this case, where the loops cross each other at 10 Hz. The figure plots  $C_1 P_1$  in blue,  $C_2 P_2$  in green and the sum  $C_1 P_1 + C_2 P_2$  in red. Ultimately it is the red curve that matters for stability.

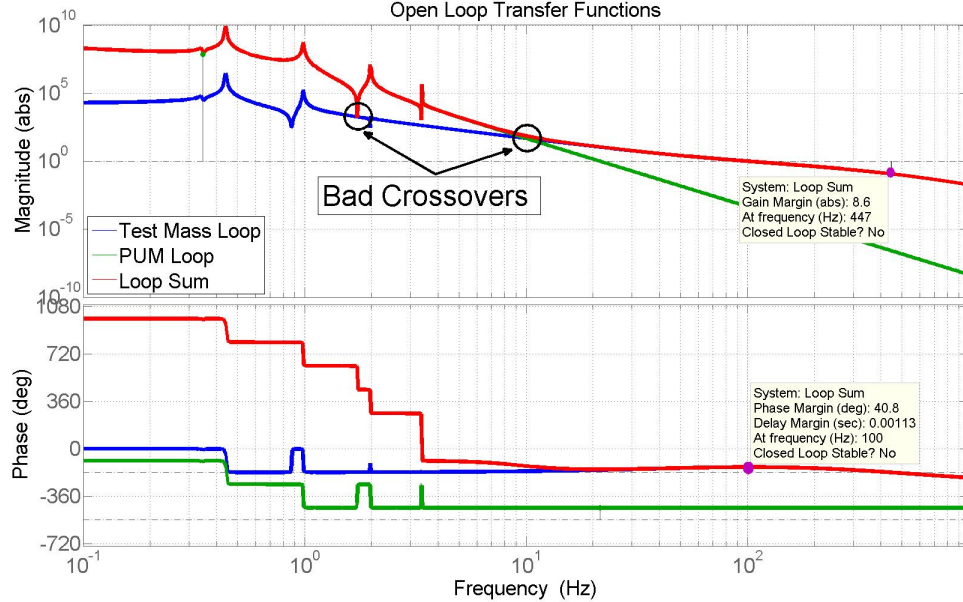


Figure 9: The open loop transfer functions for feedback to both the test mass and PUM. The blue curve is the open loop transfer function,  $C_1 P_1$ , of the test mass controller. The green curve is the open loop transfer function,  $C_2 P_2$ , of the PUM controller. The red curve is the overall sum of the two. The closed loop system is unstable.

At first glance this loop might look stable because when the red curve crosses unity gain it has good phase margin and when it crosses  $-180$  degrees it has good gain margin. However, when the green curve crosses the blue curve the relative phase between the two is more than

$-180$  degrees, which causes the closed loop to go unstable. This instability is reflected by Matlab in the phase plot by the fact that the red curve does not follow the green curve below  $10$  Hz where the green magnitude is greatest. If we were to shift the red phase curve by multiples of  $360$  degrees such that it starts at the same phase as the green, we would see that in fact the red phase curve does cross  $-180$  degrees while the gain was still greater than unity.

If we redesign the PUM controller  $C_2$  to increase the phase margin of  $C_2P_2$  where it crosses the test mass loop  $C_1P_1$  we can make this system stable. So, we do away with the integrating pole at  $0$  Hz, and add a zero at  $1$  Hz to boost the phase. Then two poles at  $100$  Hz are added to roll the controller gain off at high frequencies where we do not need it. The loop crossover is increased to  $20$  Hz to boost the low frequency gain to make up some of what was lost from throwing away the integrating pole.

The new stable loop transfer functions are plotted in Figure 10. Note that the red phase curve now follows both the blue and green curves wherever the magnitude is greatest. Additionally, the PUM loop increases the low frequency gain of the overall controller by about a factor of  $20$ , rejecting seismic noise by an equivalent amount.

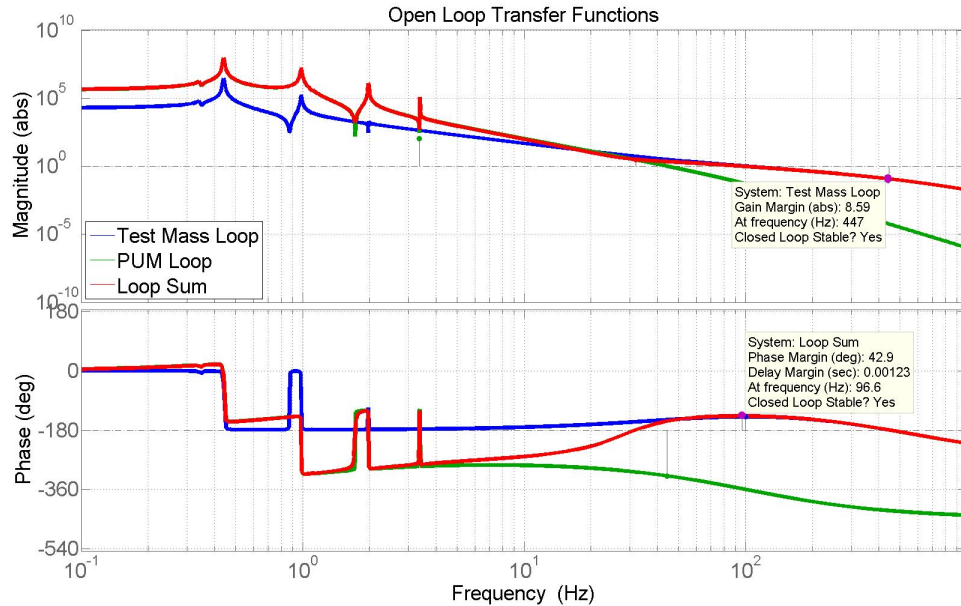


Figure 10: The open loop transfer functions for feedback to both the test mass and PUM. The blue curve is the open loop transfer function,  $C_1P_1$ , of the test mass controller. The green curve is the open loop transfer function,  $C_2P_2$ , of the PUM controller. The red curve is the overall sum of the two. The closed loop system is stable.

A more obvious way to show stability margins where the loops cross each other is to plot the loop gain transfer function given by Eq. 8. Figure 11 plots the approximate transfer function  $\frac{C_2P_2}{C_1P_1}$  and shows the stability margins. This approximation is only accurate where the test mass loop is greater than unity. Conveniently, where the approximation is valid is the only place it matters when considering the loop crossovers.

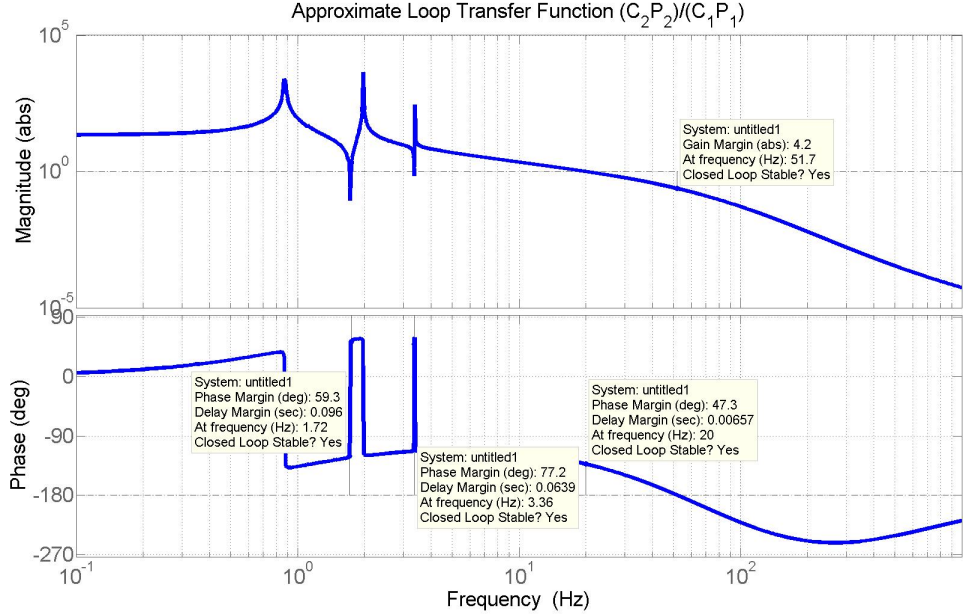


Figure 11: The stable open loop transfer function plotted as the ratio of the two component loop gains.

Representing the loop transfer function as the ratio of the two loops can simplify the design of the upper stage loops because gain and phase margins can be read directly off the plots. Additionally, this ratio leads us to another simplification that benefits the practical implementation of these loops on a real system. To this end, let's rewrite  $C_2$  as a modified version  $C'_2$ . So now

$$C'_2 = C_1 C_2 \quad (13)$$

and the approximate loop transfer function ratio becomes

$$\frac{C'_2 P_2}{C_1 P_1} = C_2 \frac{P_2}{P_1} \quad (14)$$

Forcing  $C'_2$  to be a function of  $C_1$  gives us a more robust design in the sense that if we ever choose to modify  $C_1$ , we do not have to redesign  $C_2$  to have stable crossovers because any modifications are automatically passed to  $C'_2$ . In practice, implementing this constraint is extremely easy because all it entails is sending the PUM controller the output of the test mass controller instead of the input. The modified block diagram is given in Figure 12.

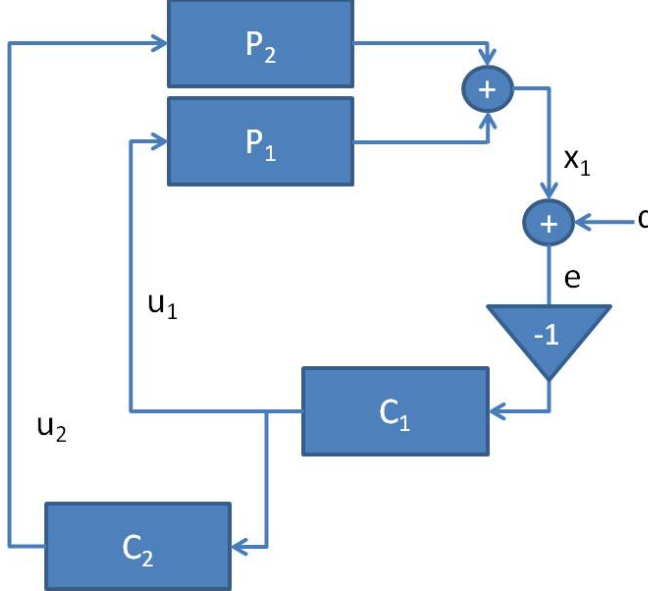


Figure 12: The block diagram is modified to implement the robust modification, given by Eq. 14, that feedback to the PUM become a function of feedback to the test mass. The input to the PUM controller is now the output of the test mass controller. In this way modifying  $C_1$  has no impact on the stability margins where the magnitude of the PUM loop crosses the magnitude of the test mass loop.

### 3.2 Generalization to N Inputs

There is no change in hierarchical control theory by extending it to an arbitrary number of inputs. The primary considerations here are robustness and practicality of implementation on a real system.

As discussed for the two input case, we can examine the stability margins for the crossover of two loops with gains greater than 1 by plotting the ratio of the two loops. However, if more than two loops cross very close to each other, then all bets are off. Additionally, such a feedback system is not likely to be robust. It is more practical to design a feedback system, and guarantee robustness if the loop crossovers are maintained at some distance from each other. A design such as this also enables use of the simplifying features of passing the output of one controller to the input of the next controller as discussed at the end of Section 3.1.

To illustrate these points let's consider feedback to all four stages of a quadruple pendulum. The closed loop transfer function we get by invoking the simplification of Eqs. 13 and 14 is

$$\frac{e}{d} = \frac{1}{1 + C_1 P_1 + C_1 C_2 P_2 + C_1 C_2 C_3 P_3 + C_1 C_2 C_3 C_4 P_4} \quad (15)$$

Factoring like terms gives us

$$\frac{e}{d} = \frac{1}{1 + C_1 P_1 \{1 + C_2 \frac{P_2}{P_1} [1 + C_3 \frac{P_3}{P_2} (1 + C_4 \frac{P_4}{P_3})]\}} \quad (16)$$

If all the loop crossovers are sufficiently separated from each other then there is one independent stability criterion for each input. Conveniently, each criterion is very reminiscent of the SISO case. So in this case the four instability criterion for Eq. 16 are

$$C_1 P_1 = -1 \quad (17)$$

$$C_2 \frac{P_2}{P_1} = -1 \quad (18)$$

$$C_3 \frac{P_3}{P_2} = -1 \quad (19)$$

$$C_4 \frac{P_4}{P_3} = -1 \quad (20)$$

Phase and gain margins can independently be read off Bode plots of each of the four transfer functions in these criteria. Each controller can then be designed independently. In the same way, if a controller to one stage is changed at a later time, the others do not need to be reevaluated for stability.

Though these approximations are highly useful, it is still good practice to double check overall stability by plotting the phase and gain of the sum of the loops,  $C_1 P_1 + C_1 C_2 P_2 + C_1 C_2 C_3 P_3 + C_1 C_2 C_3 C_4 P_4$  to ensure that they all work together as desired.